ASEAN
Journal of Scientific and Technological Reports
Online ISSN:2773-8752

Research article

Statistical Analysis of CAPWAP-Derived Settlement Considering Pile Resistance Components and Geometry: A Bored-Pile Case Study in Jakarta

Tri Susanto[1*], Hanggoro Iskandar Putra Wijaya[1], and Bambang Setiabudi[1]

[1] Department of Civil and Planning, Universitas Diponegoro, Indonesia
* Correspondence: tsusanto@live.undip.ac.id

Citation:
Susanto, T.; Wijaya, H.I.P.; Setiabudi, B. Statistical analysis of CAPWAP-Derived settlement considering pile resistance components and geometry: A bored-pile case study in Jakarta. *ASEAN J. Sci. Tech. Report.* **2026** *29*(12), e260830. https://doi.org/10.55164/ajstr.v29i12.260830

Article history:
Received: August 13, 2025
Revised: August 13, 2026
Accepted: Septem 27, 2026
Available online: November 22, 2026

Publisher's Note:
This article is published and distributed under the terms of the Thaksin University.

Abstract: High-strain dynamic testing provides rapid estimates of mobilized pile resistance and associated pile-head movement, but CAPWAP-derived displacement should not be interpreted as long-term static settlement. This study evaluates thirteen bored piles from an anonymized Jakarta project, with diameters of 1,200-1,500 mm and lengths of 17.00-43.00 m. CAPWAP outputs were analyzed for total pile resistance, skin friction, end-bearing resistance, and reported settlement using simple and exploratory multiple linear regression, residual diagnostics, and influence analysis. Pile resistance showed a positive association with CAPWAP-derived settlement ($R^2 = 0.7101$, $F = 26.94$, $p = 0.0003$), while skin friction was also associated with settlement ($R^2 = 0.6339$, $p = 0.0011$). End-bearing resistance alone showed no linear association ($R^2 = 0.0009$, $p = 0.9215$). An exploratory model including pile resistance, length, and diameter explained 79.7% of the observed variation (adjusted $R^2 = 0.7296$), although only pile resistance was statistically significant ($p = 0.0066$). Influence analysis identified P177' as highly influential (Cook's D = 4.08); removing this point reduced R^2 to 0.3502. Residual normality was acceptable (Shapiro-Wilk $p = 0.854$), with no significant evidence of heteroscedasticity in the primary model (Breusch-Pagan $p = 0.066$). Because n = 13, soil-profile data and static load-test settlement were unavailable; the results are project-specific and exploratory.

Keywords: CAPWAP; high-strain dynamic testing; bored pile; shaft resistance; pile settlement

1. Introduction

Deep foundations are commonly used where near-surface soils cannot safely support structural loads, and their performance depends on the interaction among pile geometry, soil resistance, installation conditions, and applied loading [1–3]. For bored piles, axial resistance is mobilized through shaft resistance and toe resistance, while pile-head movement develops as the pile-soil system responds to loading [4–14]. Field verification is therefore important because resistance estimated from design-stage SPT or CPT data may differ from the resistance mobilized during construction-stage testing [1, 15–17]. The present study uses construction-stage high-strain dynamic test records from an anonymized urban project in Jakarta, Indonesia, reported as Project X.

High-strain dynamic testing under ASTM D4945 measures the force and velocity response generated by an axial impact on a deep foundation element [18]. For cast-in-place or bored piles, the test is performed after pile construction and pile-head preparation by applying a controlled impact; it is not a pile-driving operation. The measured force-velocity signals can be interpreted

directly and can also be subjected to CAPWAP signal matching. In CAPWAP, a wave-equation model of the pile-soil system is iteratively adjusted until the calculated response is consistent with the measured signal, providing estimates of mobilized total resistance and its shaft and toe components [3, 19–22]. These outputs are indirect dynamic-test estimates and depend on the mobilized soil response, test energy, signal quality, and the assumptions adopted in the signal-matching model [18, 20–22].

The relative contributions of skin friction and end-bearing resistance are important because piles with similar total resistance may mobilize different resistance mechanisms [4–6, 20]. Pile length and diameter also affect available shaft area, toe area, stiffness, and the magnitude of resistance that can be mobilized [8, 9, 12, 14, 23]. Accordingly, an observed relationship between total resistance and movement can be confounded by pile geometry and by site-specific soil conditions. Evaluating resistance components and geometry together is therefore more informative than interpreting total pile resistance alone.

A further distinction is required between movement reported during a high-strain dynamic event and the static, time-dependent settlement used for serviceability design. ASTM D4945 identifies mobilized compressive static resistance derived from dynamic measurements as an indirect result, whereas static load testing directly measures load-displacement response under static loading [18]. CAPWAP interpretation can provide useful resistance distribution and movement information, but setup effects, residual loads, and other soil-pile interaction factors can affect comparison with static behavior [20]. Therefore, the term 'settlement' in this manuscript refers specifically to the CAPWAP-reported pile-head displacement from the dynamic test record and is not treated as a prediction of long-term service settlement.

This study aims to (1) quantify the project-specific statistical association between CAPWAP total pile resistance and CAPWAP-derived settlement; (2) evaluate the separate relationships of skin friction, end-bearing resistance, pile length, and pile diameter with the reported settlement; and (3) examine regression assumptions and influential observations to determine how strongly individual test points affect the apparent trend. The study is intentionally interpreted as an exploratory single-project analysis because only thirteen test locations are available and the analytical dataset does not include project-specific soil profiles or static load-test settlement records.

2. Materials and Methods

2.1 Study scope and data source

The dataset comprises thirteen bored-pile test locations from Project X in Jakarta. The analyzed records contain pile diameter, pile length, CAPWAP total pile resistance (PR), skin friction or shaft resistance (SF), end-bearing resistance (EBC), and CAPWAP-reported settlement. Pile diameters are 1,200 or 1,500 mm and pile lengths range from 17.00 to 43.00 m (Table 1). The case is retained as Project X because the source records used for this analysis are anonymized; the analytical dataset available for this manuscript does not specify the facility subtype or construction year. Consequently, the findings are restricted to the tested piles and are not intended to represent all bored-pile foundations in Jakarta.

2.2 Geotechnical context and scope limitation

Project-specific borehole logs, soil stratigraphy, SPT profiles, groundwater records, and laboratory soil parameters were not included in the archived PDA/CAPWAP dataset used in this study. Therefore, between-pier differences cannot be quantitatively assigned to particular soil layers [10, 11, 14]. Soil heterogeneity is treated as an unobserved source of variability rather than being inferred from resistance data. This limitation is explicitly considered when interpreting the statistical results and prevents geotechnical generalization beyond Project X.

2.3 High-strain dynamic testing and CAPWAP analysis

The testing framework follows the principles of ASTM D4945 [18]. During a high-strain impact event, strain/force and acceleration-derived velocity responses are recorded near the pile head. For bored piles, the impact is applied after pile installation; sufficient impact energy is required to mobilize soil resistance without interpreting the test as conventional pile driving. The source dataset supplied to this study contains the processed PDA/CAPWAP results rather than the complete raw force-velocity time histories; consequently,

instrumentation serial numbers, exact impact energies, and operator-specific matching settings cannot be independently reconstructed from the archived dataset. CAPWAP uses signal matching to reproduce the measured wave response with a numerical pile-soil model. The resistance distribution is adjusted along the shaft and at the toe together with dynamic soil parameters until an acceptable match is obtained [3, 19–22]. The reported total pile resistance is treated as the sum of the mobilized shaft and toe components, PR = SF + EBC. The ratios SF/PR and EBC/PR are used to describe the relative contribution of each mechanism. The movement variable analyzed in this manuscript is the CAPWAP-reported settlement associated with the dynamic test and is distinguished from long-term static service settlement.

Table 1. Bored-pile geometry at the thirteen PDA/CAPWAP test locations in Project X, Jakarta

Pier	Foundation	Pile Dimension (mm)	Pile Length (m)
P7	Bore Pile	1200	28.00
P55	Bore Pile	1200	29.50
P55'	Bore Pile	1200	28.00
P10	Bore Pile	1200	30.10
P148	Bore Pile	1200	17.00
P153	Bore Pile	1200	17.00
P157	Bore Pile	1200	22.40
P162	Bore Pile	1500	30.00
P177	Bore Pile	1200	43.00
P184	Bore Pile	1200	27.00
P140	Bore Pile	1200	27.00
P162'	Bore Pile	1500	30.00
P177'	Bore Pile	1500	43.00

2.4 Statistical analysis

Statistical analysis was conducted using the thirteen test locations as observational units. First, simple linear regressions were evaluated for CAPWAP-derived settlement versus PR, SF, EBC, and pile length; the two diameter groups (1,200 and 1,500 mm) were also compared within a linear-model framework. For the primary PR-settlement regression, the coefficient of determination (R^2), F-statistic, and p-value were reported. Residual normality was assessed using the Shapiro-Wilk test, and constant variance was evaluated using the Breusch-Pagan test together with a residual-versus-fitted plot. Influence was examined using leverage, externally studentized residuals, and Cook's distance; because n = 13, the results were interpreted cautiously. A sensitivity regression excluding the most influential point was also calculated. Finally, two exploratory multiple linear models were evaluated: Model A included PR, pile length, and a diameter-group indicator; Model B replaced PR with SF and EBC while retaining length and diameter. These multivariable models are descriptive/exploratory rather than predictive because of the small sample size. Statistical significance was evaluated at $\alpha = 0.05$, but effect size, influence diagnostics, and engineering plausibility were considered together rather than relying on p-values alone.

3. Results and Discussion

The CAPWAP results for total pile resistance, skin friction, and end-bearing resistance are summarized in Table 2 and Figure 1. Figure 2 compares the CAPWAP-reported settlement with the source-reported quantity labeled 'Fixed Settlement.' Table 3 and Figure 3 present the primary relationship between pile resistance and CAPWAP-derived settlement. Additional regressions for resistance components and geometry are summarized in Table 4 and Figures 4-5, while the primary regression residuals are shown in Figure 6.

Table 2. Comparison of pile resistance, skin friction, and end bearing capacity

Pier	Pile Resistance (PR)	Skin Friction (SF)		End Bearing Capacity (EBC)	
	(Tons)	(Tons)	SF/PR	(Tons)	EBC/PR
P7	841.50	689.30	81.91%	152.2	18.09%
P55	953.10	811.90	85.19%	141.20	14.81%
P55'	1296.20	1184.90	91.41%	111.30	8.59%
P10	1416.80	1353.10	95.50%	63.70	4.50%
P148	1015.90	638.90	62.89%	377.00	37.11%
P153	1266.70	891.70	70.40%	375.00	29.60%
P157	1375.40	1276.00	92.77%	99.40	7.23%
P162	1498.00	1399.50	93.42%	98.50	6.58%
P177	1228.70	1132.30	92.15%	96.40	7.85%
P184	1168.50	1055.20	90.30%	113.30	9.70%
P140	1185.40	1132.00	95.50%	53.40	4.50%
P162'	1450.50	1336.80	92.16%	113.70	7.84%
P177'	2012.20	1762.60	87.60%	249.60	12.40%

Table 2 shows that shaft resistance dominates total mobilized resistance at most locations. Eleven of the thirteen piles have SF/PR values above 80%, indicating that the CAPWAP resistance distribution is predominantly shaft-controlled for these test records. P148 and P153 are the exceptions, with end-bearing contributions of 37.11% and 29.60%, respectively. Both piles are 17.00 m long, whereas the remaining piles are 22.40-43.00 m long. The observation is consistent with the general expectation that pile geometry and the soil profile encountered along the shaft and at the toe can alter the relative resistance mechanism [19-24]. Because project-specific stratigraphy is unavailable, however, the higher EBC/PR values at P148 and P153 cannot be attributed to a specific bearing layer and should be treated as a project-level observation rather than a soil-mechanism proof.

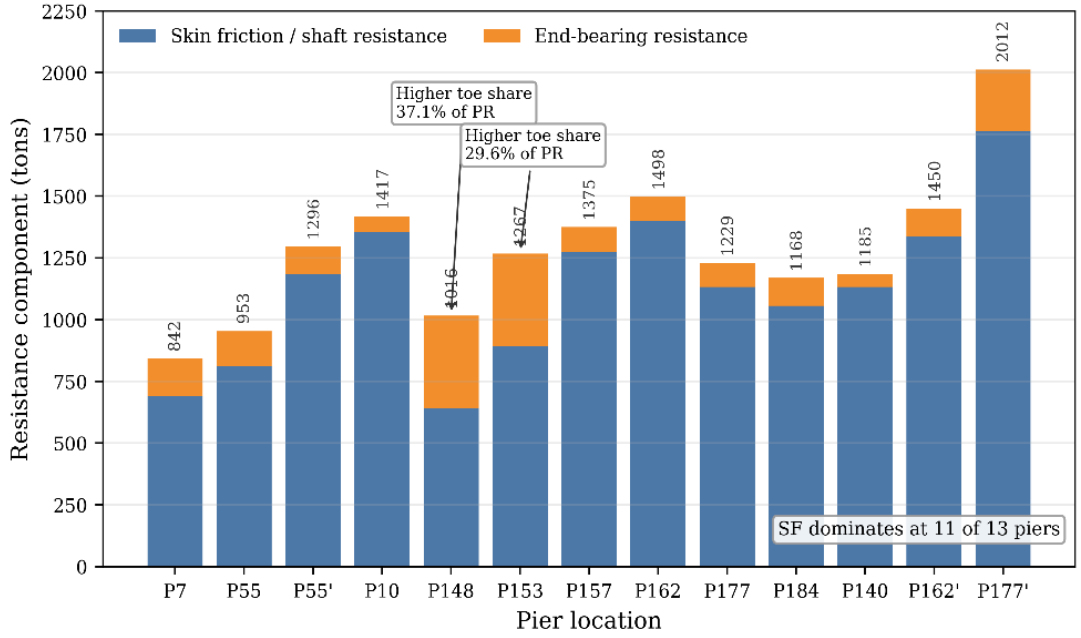

Figure 1. Comparison of pile resistance, skin friction, and end-bearing resistance

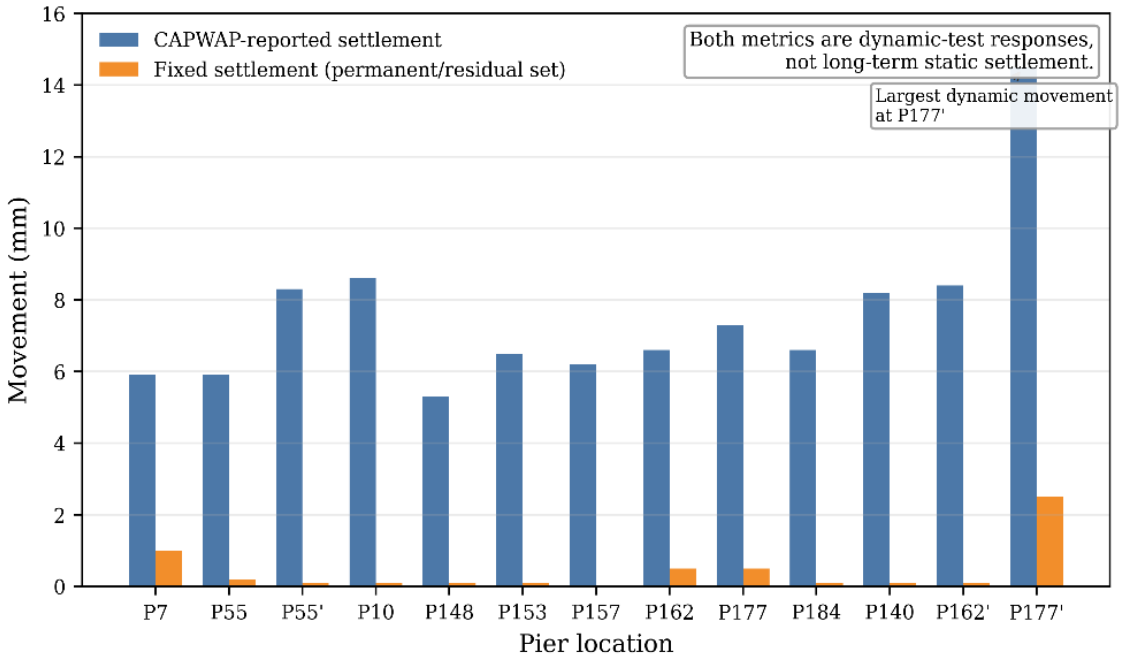

Figure 2. Comparison of settlement and fixed settlement

The source test records distinguish 'Settlement' from 'Fixed Settlement' (Figure 2). In this manuscript, 'Fixed Settlement' is defined as the permanent or residual pile-head set reported after the dynamic impact event, whereas 'Settlement' is the larger CAPWAP-reported movement associated with the event. Both are dynamic-test response quantities; neither is interpreted as long-term static service settlement. The largest reported settlement is 14.50 mm at P177', which is also the longest pile group (43.00 m) and has the largest total resistance (2,012.20 tons). This combination suggests that the observed movement reflects the amount of resistance mobilized during impact as well as pile geometry and soil-pile response, rather than a simple serviceability relation in which greater capacity necessarily implies smaller settlement.

Table 3. Comparison of pile resistance and CAPWAP-derived settlement.

Pier	Pile Resistance (Tons)	Settlement (mm)
P7	841.50	5.90
P55	953.10	5.90
P55'	1296.20	8.30
P10	1416.80	8.60
P148	1015.90	5.30
P153	1266.70	6.50
P157	1375.40	6.20
P162	1498.00	6.60
P177	1228.70	7.30
P184	1168.50	6.60
P140	1185.40	8.20
P162'	1450.50	8.40
P177'	2012.20	14.50

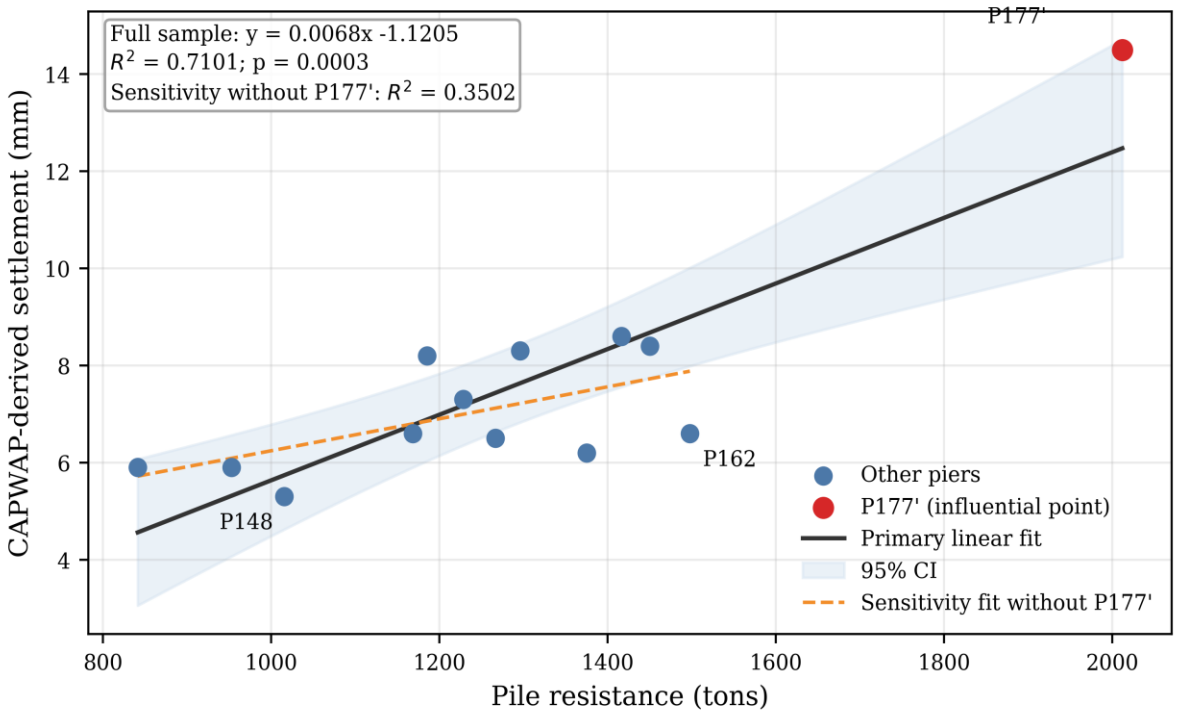

Figure 3. CAPWAP-derived settlement versus pile resistance with simple linear regression

Across all thirteen tests, pile resistance is positively associated with CAPWAP-derived settlement (Figure 3). The fitted equation is y = 0.00675x - 1.12045, with R^2 = 0.7101, F(1,11) = 26.94, and p = 0.0003. The regression therefore describes a statistically detectable association within this dataset, but it should not be interpreted as a universal physical law. The negative intercept (-1.12 mm at zero resistance) is physically meaningless and demonstrates that the linear model is valid only within the observed resistance range; it must not be extrapolated toward zero load or used as a general settlement-prediction equation. Influence diagnostics identify P177' as highly influential (leverage = 0.588, externally studentized residual = 3.284, Cook's D = 4.076). When P177' is excluded as a sensitivity check, the fitted relationship weakens substantially to y = 0.00329x + 2.953, R^2 = 0.3502, although the slope remains significant at p = 0.0427. This sensitivity confirms the reviewer's concern that the apparent strength of the full-sample regression is strongly affected by one observation.

Table 4. Univariate relationships with CAPWAP-derived settlement

Predictor	Slope/effect	R^2	F	p
Pile resistance (tons)	0.00675 mm/ton	0.7101	26.94	0.0003
Skin friction (tons)	0.00595 mm/ton	0.6339	19.05	0.0011
End bearing (tons)	-0.00066 mm/ton	0.0009	0.01	0.9215
Pile length (m)	0.1960 mm/m	0.4253	8.14	0.0157
Diameter group	+2.953 mm (1500 vs 1200)	0.3031	4.78	0.0512

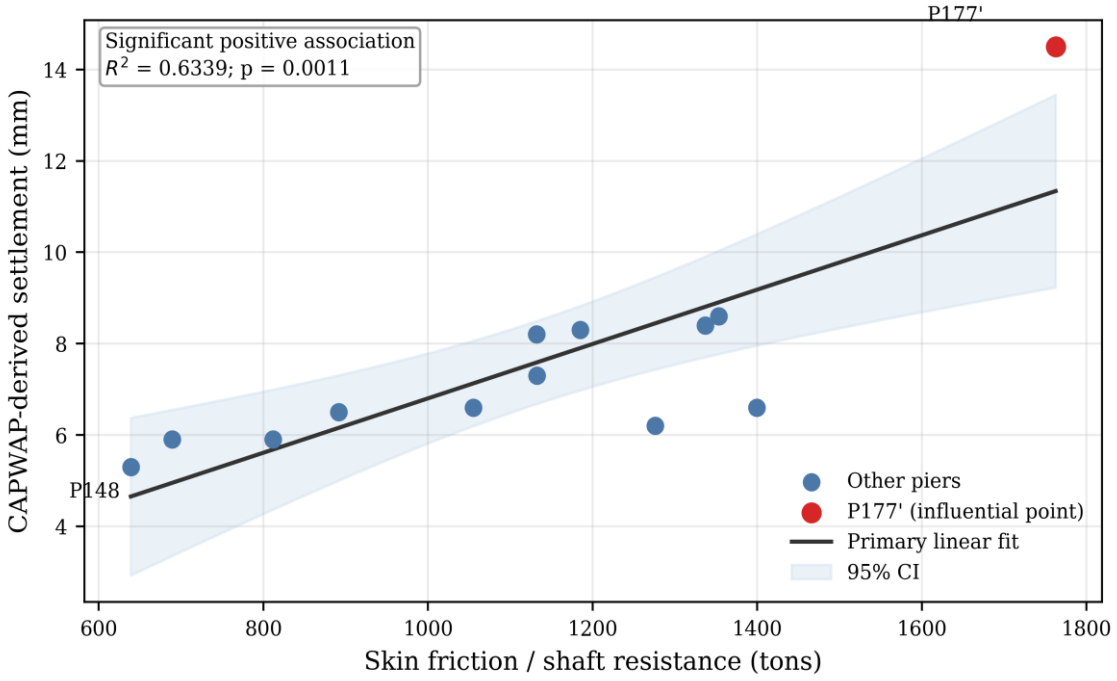

Figure 4. CAPWAP-derived settlement versus skin friction (shaft resistance)

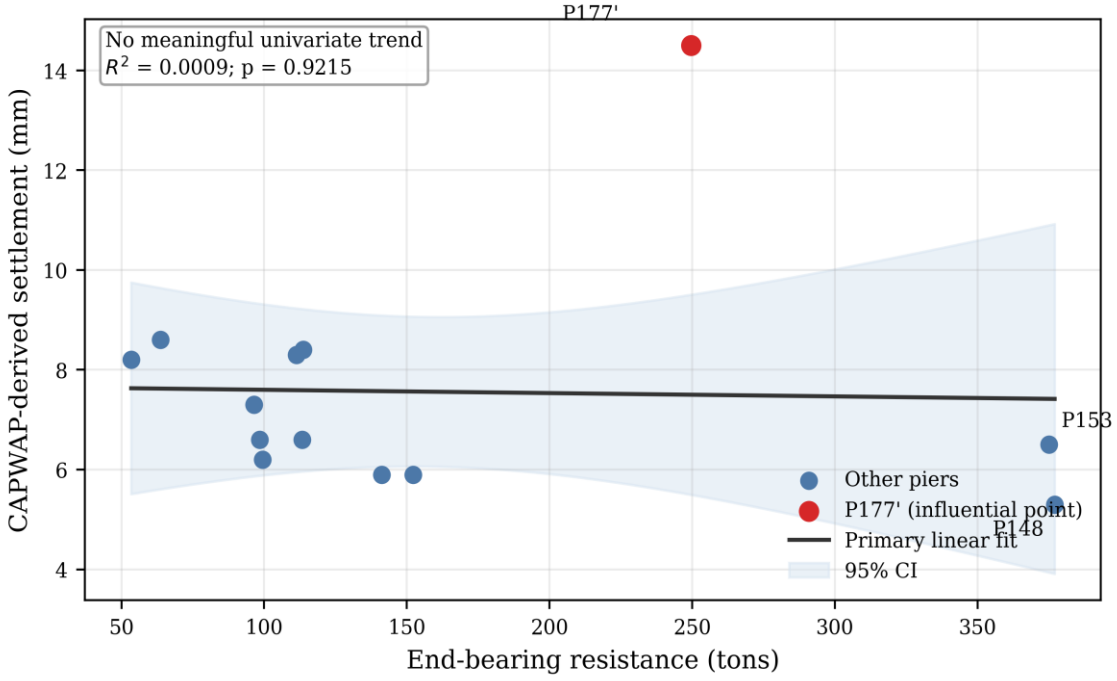

Figure 5. CAPWAP-derived settlement versus end-bearing resistance

The component-level analysis shows that skin friction has a significant positive univariate association with the CAPWAP-derived settlement (R^2 = 0.6339, p = 0.0011; Figure 4), whereas end-bearing resistance has essentially no univariate linear association (R^2 = 0.0009, p = 0.9215; Figure 5). Pile length also shows a positive univariate association (R^2 = 0.4253, p = 0.0157), while the difference between the 1,500-mm and 1,200-mm diameter groups is not significant at α = 0.05 (p = 0.0512). These simple regressions are not independent causal effects because the predictors co-vary across the same thirteen piles. In exploratory Model A (PR + length + diameter group), R^2 = 0.7972 and adjusted R^2 = 0.7296 with an overall p = 0.0018; PR remains significant (coefficient = 0.00634 mm/ton, p = 0.0066), while length (p = 0.0896) and diameter group (p = 0.4991) do not. In

Model B (SF + EBC + length + diameter group), $R^2 = 0.8162$ and adjusted $R^2 = 0.7243$ with an overall $p = 0.0049$; SF ($p = 0.0109$) and EBC ($p = 0.0417$) are significant within that model, whereas length and diameter are not. Because Model B uses four predictors with only thirteen observations and P177' remains influential, these coefficients are interpreted only as exploratory evidence of interacting resistance mechanisms rather than a stable predictive model.

Table 5. Exploratory multiple linear regression results

Model	Predictor	Coefficient	p
A	Pile resistance	0.00634	0.0066
A	Pile length	0.09895	0.0896
A	Diameter 1500 mm	-0.81667	0.4991
B	Skin friction	0.00609	0.0109
B	End bearing	0.00949	0.0417
B	Pile length	0.12480	0.0701
B	Diameter 1500 mm	-0.87310	0.4778

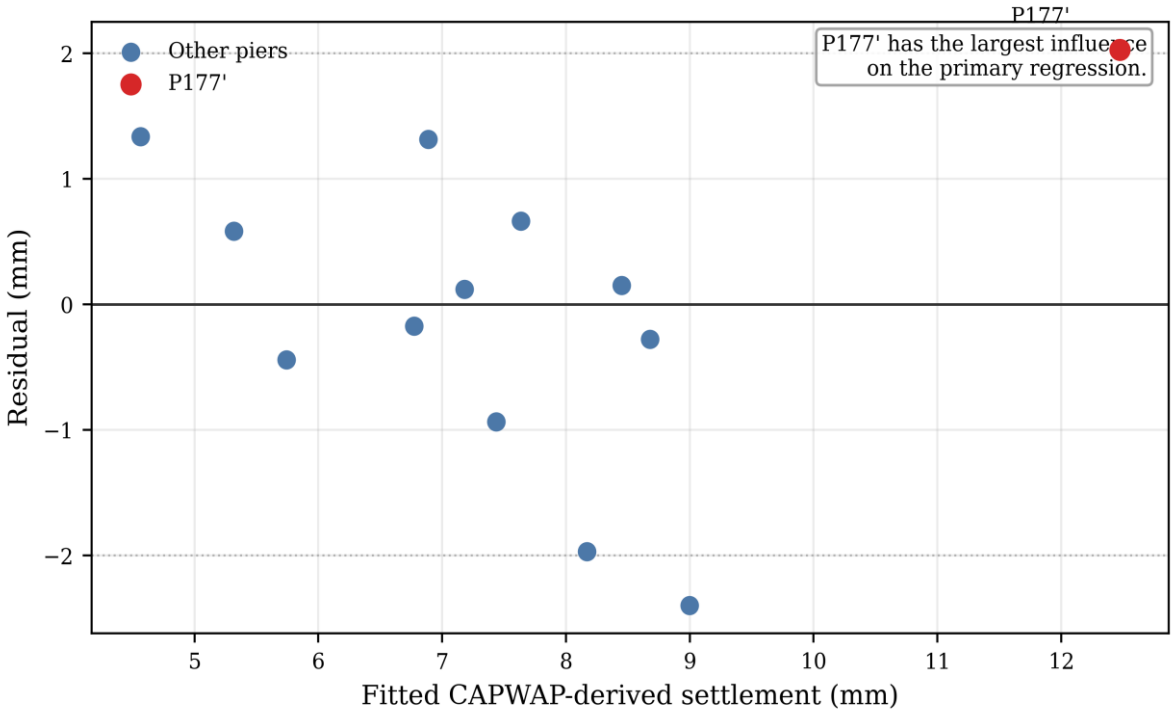

Figure 6. Residual-versus-fitted plot for the primary pile-resistance regression

For the primary regression, the residuals do not depart significantly from normality (Shapiro-Wilk $W = 0.9669$, $p = 0.8544$). The Breusch-Pagan test gives $p = 0.0659$, so there is no statistically significant evidence of heteroscedasticity at $\alpha = 0.05$, although the small sample provides limited diagnostic power. The residual plot in Figure 6 and the influence statistics nevertheless show that P177 warrants special attention. Independence was assumed at the pier level for the regression calculation, but spatial dependence among piles within one project cannot be ruled out. These diagnostics reinforce that the regression is descriptive for this case study and should not be generalized without a larger dataset, project-specific soil profiles, and preferably static load-test measurements for external validation [21, 22, 24].

4. Conclusions

The thirteen CAPWAP records show that mobilized bored-pile resistance in Project X is predominantly shaft-controlled: eleven piles have SF/PR ratios greater than 80%, while P148 and P153 show

larger toe-resistance contributions of 37.11% and 29.60%. A statistically significant positive association is observed between total pile resistance and CAPWAP-derived settlement (R^2 = 0.7101, p = 0.0003), but the relationship is strongly influenced by P177. Excluding this point reduces R^2 to 0.3502, demonstrating that the full-sample regression is not sufficiently robust for general prediction. Skin friction is significantly associated with the reported movement in univariate analysis, whereas end-bearing resistance alone is not; exploratory multivariable models further indicate that resistance components and geometry should be considered together. The negative intercept of the primary regression has no physical meaning, and the model must not be extrapolated beyond the observed data range. Most importantly, the settlement variable analyzed here is a CAPWAP-derived dynamic pile-head movement, not long-term static service settlement. Because the study is based on only thirteen piles from one anonymized project and lacks project-specific soil profiles and static load-test settlement data, the results should be treated as project-specific exploratory evidence. Future work should combine a larger multi-project dataset with stratigraphy/SPT information, groundwater conditions, pile geometry, raw dynamic-test signals, and static load tests to evaluate the transferability of these relationships.

5. Acknowledgments

The authors would like to thank the support provided by the Department of Civil and Planning, Vocational College, Universitas Diponegoro, Indonesia.

Author Contributions: Conceptualization, T.S. and H.I.P.W.; methodology, T.S.; software, T.S.; validation, H.I.P.W., T.S. and B.S.; formal analysis, T.S.; investigation, B.S. and H.I.P.W.; resources, T.S.; data curation, B.S.; writing—original draft preparation, H.I.P.W. and T.S.; writing—review and editing, T.S. and B.S.; visualization, H.I.P.W.; supervision, B.S.; project administration, H.I.P.W.; funding acquisition, B.S. All authors have read and agreed to the published version of the manuscript.

Funding: The authors would like to thank Universitas Diponegoro for providing a grant for this research. This research was financially supported by Vocational College, Universitas Diponegoro, Indonesia, through Research Grant (DIPA) 2025.

Conflicts of Interest: The study's design, methodology, data analysis, and results were all independent of the funding agency; therefore, the authors report no conflicts of interest.

References

[1] Santoso, H. T.; Hartono, J. Analisis Perbandingan Daya Dukung Pondasi Tiang Pancang Berdasar Hasil Uji SPT dan Pengujian Dinamis. **2020**. https://doi.org/10.20961/jrrs.v4i1.44635

[2] Hardiyatmo, H. C. *Analisis dan Perancangan Fondasi II*, 5th ed.; UGM Press: Yogyakarta, Indonesia, **2022**.

[3] Fellenius, B. H. *Basics of Foundation Design*, Electronic ed.; British Columbia, Canada, **2023**.

[4] Maralapalle, V. C.; Nadaf, M. B.; Dutta, S.; Zende, A. A.; Mishra, S. S.; Charhate, S. Load-Settlement and Skin Friction Behaviour of Piles in Dry Sand: Experimental and Numerical Study. *Sādhanā* **2023**, *49*(1), 4. https://doi.org/10.1007/s12046-023-02362-2

[5] Siemaszko, P.; Meyer, Z. Analysis of the Pile Skin Resistance Formation. *Stud. Geotech. Mech.* **2021**, *43*(4), 380–388. https://doi.org/10.2478/sgem-2021-0026

[6] Alzabeebee, S.; Chapman, D. N. Evolutionary Computing to Determine the Skin Friction Capacity of Piles Embedded in Clay and Evaluation of the Available Analytical Methods. *Transp. Geotech.* **2020**, *24*, 100372. https://doi.org/10.1016/j.trgeo.2020.100372

[7] Chai, Q.; Chen, T.; Li, Z.; Shen, D.; Wu, C. Experimental Study on the Negative Skin Friction of Piles in Collapsible Loess. *Sustainability* **2023**, *15*(11), 8893. https://doi.org/10.3390/su15118893

[8] Nguyen, T. T.; Le, V. D.; Huynh, T. Q.; Nguyen, N. H. T. Influence of Settlement on Base Resistance of Long Piles in Soft Soil—Field and Machine Learning Assessments. *Geotechnics* **2024**, *4*(2), 447–469. https://doi.org/10.3390/geotechnics4020025

[9] Rivera, N. E.; Estores, G. B. Single Pile FEM Modeling: Ultimate Capacity Determination of Bored Piles Embedded in Silty-Sands Using Modified Drucker-Prager Cap Model. *Civil Eng. Archit.* **2022**, *10*(1), 175–193. https://doi.org/10.13189/cea.2022.100116

[10] Ong, Y. H.; Toh, C. T.; Chee, S. K.; Mohamad, H. Bored Piles in Tropical Soils and Rocks: Shaft and Base Resistances, t-z and q-w Models. *Proc. Inst. Civ. Eng.—Geotech. Eng.* **2021**, *174*(2), 193–224. https://doi.org/10.1680/jgeen.19.00106

[11] Ma, D.; Zhang, M.; Shi, Y.; Zhu, W. Analysis of Load-Settlement Curve Based on Load Transfer at Pile-Soil Interface. *Appl. Sci.* **2022**, *12* (14), 7150. https://doi.org/10.3390/app12147150

[12] Li, Y.; Zhu, X.; Chen, L.; Zhou, T. Load Transfer Calculation and Analysis of Large-Diameter Bored Piles According to Rules Based on Test Pile Measurement. *J. Highw. Transp. Res. Dev. (Engl. Ed.)* **2018**, *12*(3), 28–36. https://doi.org/10.1061/JHTRCQ.0000637

[13] Comodromos, E. M.; Randolph, M. F. Improved Relationships for the Pile Base Response in Sandy Soils. *J. Geotech. Geoenviron. Eng.* **2023**, *149*(8), 04023058. https://doi.org/10.1061/JGGEFK.GTENG-11035

[14] Cesaro, R.; Di Laora, R.; Mandolini, A. Shaft Resistance of Bored Piles in Sand. *Acta Geotech.* **2026**, *21*, 3103–3126. https://doi.org/10.1007/s11440-025-02860-z

[15] Sari, U. C.; Mirza Abdillah Pratama, M.; Atpriyanti, D. N.; Negoro, N. A. The Bearing Capacity Analysis of Deep Foundation Based on In-Situ Dynamic Penetration Test Compared to Pile Driving Analyzer (PDA). *IOP Conf. Ser.: Earth Environ. Sci.* **2023**, *1203*(1), 012017. https://doi.org/10.1088/1755-1315/1203/1/012017

[16] Prativi, A.; Dewi, P.; Sutra, N.; Adi, W. T.; Weijia, C. Comparison of Individual Bored Pile Bearing Capacity Using the Results of Standard Penetration Test (SPT) and Pile Driving Analysis (PDA) Test of the Railway Bridge Foundation. *J. Railw. Transp. Technol.* **2022**, *1*(2), 14–23. https://doi.org/10.37367/jrtt.v1i2.9

[17] Zulfiqar, M.; Hudori, M. Studi Komparatif Daya Dukung Pondasi Tiang Pancang Berdasarkan Hasil Pile Driving Analyzer Test dan N-SPT. *J. Talenta Sipil* **2023**, *6*(2), 229–235. https://doi.org/10.33087/talentasipil.v6i2.259

[18] ASTM International. *ASTM D4945-26: Standard Test Method for High-Strain Dynamic Testing of Deep Foundations*; ASTM International: West Conshohocken, PA, USA, **2026**. https://doi.org/10.1520/D4945-26

[19] Fakharian, K. A Case Study on the Application of Pile Driving Analyzer (PDA) and CAPWAP Analysis to Bearing Capacity of Piles. In *Proceedings of the Tenth International Offshore and Polar Engineering Conference*; May 28, **2000**; p ISOPE-I-00-170.

[20] Bartz, J. R.; Blatz, J. A. Interpreting CAPWAP Results for Driven Piles with Corrections for Setup and Residual Loads. *Can. Geotech. J.* **2023**, *60*(5), 718–730. https://doi.org/10.1139/cgj-2021-0430

[21] Rausche, F.; Goble, G. G.; Likins, G. E., Jr. Dynamic Determination of Pile Capacity. *J. Geotech. Eng.* **1985**, *111*(3), 367–383. https://doi.org/10.1061/(ASCE)0733-9410(1985)111:3(367)

[22] Kuei, K. C.; DeJong, J. T.; Ghafghazi, M. Prediction, Performance, and Uncertainty in Dynamic Pile Load Testing as Informed by Direct Measurements from an Instrumented Becker Penetration Test. *J. Geotech. Geoenviron. Eng.* **2020**, *146*(8), 04020067. https://doi.org/10.1061/(ASCE)GT.1943-5606.0002290

[23] Fattahi, H.; Ghaedi, H.; Malekmahmoodi, F.; Jahed Armaghani, D. Optimizing Pile Bearing Capacity Prediction: Insights from Dynamic Testing and Smart Algorithms in Geotechnical Engineering. *Measurement* **2024**, *230*, 114563. https://doi.org/10.1016/j.measurement.2024.114563

[24] ASTM International. *ASTM D1143/D1143M-26: Standard Test Methods for Deep Foundation Elements under Static Axial Compressive Load*; ASTM International: West Conshohocken, PA, USA, **2026**. https://doi.org/10.1520/D1143_D1143M-26